Emergence and Collapse of Order in Mutually Imitating Agents

Soichiro Tsuda
School of Chemistry, University of Glasgow
Glasgow, G12 8QQ, United Kingdom
and
Institute of Molecular, Cell, and Systems Biology
University of Glasgow, 126 University Place
Glasgow G12 8TA, United Kingdom
Soichiro.Tsuda@glasgow.ac.uk

A cellular automata (CA)-like model of mutually imitating agents, called imitating cellular automata (ICA), is presented. An agent of the model either imitates a behavior of neighboring agents or takes a random action to compute the next state of its own, based on elementary cellular automata (ECA) rules. When combined with another dynamic that determines an interaction distance to the neighborhood agents, ICA show complex spatiotemporal patterns and travel around between ordered and chaotic phases without being trapped in a fixed state. The patterns were robustly observed across a wide range of parameter values and also found to follow a power-law relationship.

1. Introduction

Imitation, which is defined as the copying of behavior [1], is one of the fundamental behaviors of natural life forms. It is observed at all the scales, from molecular to social, and in some cases is crucial for higher-level behavior, such as social learning. For example, at the cellular level, mirror neurons mimic firings of other neurons, and the imitation by mirror neurons is considered to be important for acquiring complex skills such as language [2]. At a higher level, bird song imitation is one of the well-known examples in animal behavior [3], and an ability to imitate adults is essential for infants to learn new tasks [4]. The stock market is a typical example of imitation at the social level. Traders in the market take the same actions as influential traders or tend to follow the mood of the market.

Along with the growing interest in the science of imitating behavior in the last decade, many theoretical models have been proposed to replicate imitation. Suzuki and Kaneko proposed a dynamical system model of mutual-imitating agents inspired by bird song imitation [5]. Artificial stock market models based on cellular automata (CA) in

https://doi.org/10.25088/ComplexSystems.24.1.75

which traders imitate others as their behavior strategy are presented in [6, 7]. Imitation behavior was employed to construct automata models in the context of complex systems in the past. At a fundamental level, Wolfram proposed probabilistic CA, in which the rule to determine the next step was specified by the probabilities of two neighbor states [8]. Mazonka proposed a computational abstract machine model that consists of two operations, referencing and bit copying, and showed that the model was Turing complete [9]. In a more generalized perspective, Adamatzky and Wuensche investigated the notion of creativity, which would be the opposite of imitation, and CA [10]. CA rules employed there were, however, elementary cellular automata (ECA) rules, which have homogeneous agents that share the same set of rules.

In contrast, here we investigate the dynamics of mutually imitating agents, which consist of heterogeneous agents. A CA-like system, called imitating cellular automata (ICA), in which the agent can either imitate other agents or take a random action, is proposed. CA provide a simple yet powerful platform to model various kinds of natural phenomena, such as physical [11], chemical [12], biological [13], and even geological systems [14, 15]. While all agents in conventional CA share a common rule to compute next states of their own, such an assumption is rather unnatural when it comes to social and behavioral dynamics, including imitating behavior. Hence, ICA are motivated by the fact that agents are heterogeneous in natural (social) systems and are intended to construct CA-like models that capture that aspect. In addition to heterogeneity in agents, we also introduce "internal dynamics" in each ICA agent, which would correspond to, for example, the thinking process. Thus, in this paper, we will discuss what kind of dynamics would emerge from a group of mutually imitating agents, as well as the interaction between the heterogeneous (external) dynamics and the internal dynamics.

2. Imitating Cellular Automata

ICA form a spatiotemporally discrete dynamical system composed of N automata cells with K states. The dynamics are defined as:

$$\mathbf{F}(t) : \{0, \dots, K-1\}^N \mapsto \{0, \dots, K-1\}^N, \tag{1}$$

where $\mathbf{F}(t) = \left(f_1^t, \dots, f_i^t, \dots, f_N^t\right)$ and t is the discrete time of the dynamics. An automaton at the i^{th} site of the ICA (hereafter referred to as the "i^{th} cell") consists of a finite state $s_i^t \in \{0, \dots, K-1\}$, neighborhood radius r, and a transition rule table $f_i^t : \{0, \dots, K-1\}^{2r+1} \mapsto$

https://doi.org/10.25088/ComplexSystems.24.1.75

$\{0, \ldots, K-1\}$. Time development of the i^{th} cell is computed as

$$s_i^{t+1} = f_i^t\left(s_{i-r}^t, \ldots, s_i^t, \ldots, s_{i+r}^t\right). \tag{2}$$

The ICA are equivalent to the conventional one-dimensional K-state CA if $f_i^t = f_j^{t'}$ holds for all $i, j \in \{0, 1, \ldots, N\}$ and $t, t' \in N$. In this paper, we focus on the simplest case, $r = 1$ and $K = 2$, which is an ICA counterpart of ECA. $N = 100$ is used in all of the following cases.

Now let us describe how f_i^t is defined. As mentioned in the previous section, of particular interest in this model is the effect of imitating behavior on the global dynamics. For this purpose, we introduce interaction radius R and define f_i^t as follows:

$$s_i^{t+1} = \begin{cases} s_j^t & \text{if } s_{i-1,i,i+1}^t = s_{j-1,j,j+1}^{t-1} \text{ and } |i-j| \le \dfrac{R}{2} \\ X & \text{otherwise,} \end{cases} \tag{3}$$

where X is a discrete random variable that gives either 0 or 1 with probability of 0.5. If two or more cell sites $j_1, j_2, \ldots$ satisfying the first condition exist, $\max(\{j_1, j_2, \ldots\})$ (i.e., the rightmost cell of the i^{th} cell within the range of $R/2$) is adopted.

In other words, f_i^t is determined with the following process (Figure 1): First, a cell checks transitions of neighborhood cells

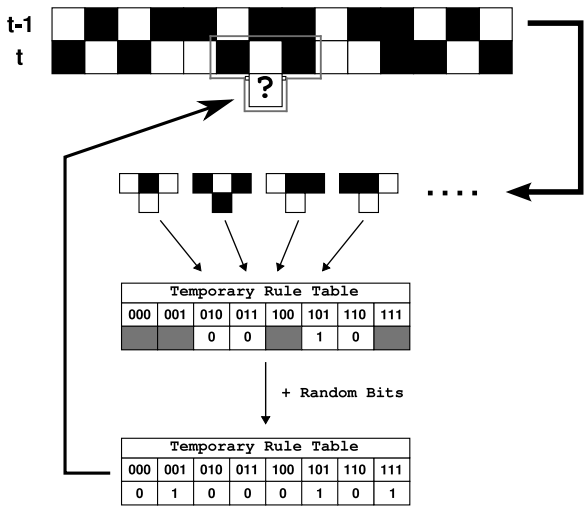

Figure 1. The schematic diagrams of ICA dynamics. Each ICA cell creates a temporary rule table from transitions of other cells made at a previous time step and applies it to compute the next state.

https://doi.org/10.25088/ComplexSystems.24.1.75

(including itself) taken at a previous time step. The interaction radius R determines the number of transitions the cell can check. Collected past transitions are put into a temporary rule table that will be used to compute the next state of the cell. If two or more transitions conflict with each other, for example, there exist $010 \to 1$ and $010 \to 0$ in a collected transition dataset, a transition from the rightmost cell triplet is adopted. Next, if the temporary rule table has blank cells, they are filled with random numbers (either 0 or 1) to complete the table. The completed temporary rule table, which is one of 256 rules of ECA, is then applied to the triplet of the current cell in order to update the cell's current state. The cell has no memory, and therefore a temporary rule table is created from scratch at every time step.

The definition of f_i^t effectively implements the following behavior of an abstract agent: (1) the agent imitates a neighboring agent if there exists the same behavior done by the neighboring agent; (2) it behaves randomly if no same behavior exists previously.

The interaction radius R is determined by another dynamic, called the intra-agent dynamic. Although any dynamic can be used in principle, one-dimensional ECA ($r = 1$ and $K = 2$) are employed here as the intra-agent dynamic of a cell in ICA (for short, "intraCA"). A temporary rule table created by the i^{th} ICA cell at time t is passed over to the intraCA and used to compute the time development of intraCA over T_{in} steps. During the computation of the time development, the input entropy $H_{\text{in}}(t)$ of the bit sequence of cells in intraCA is calculated for each time step by [16]:

$$H_{\text{in}}(t) = -\frac{1}{2r+1} \sum_{i=0}^{2^{2r+1}-1} \frac{Q_t^i}{N_{\text{in}}} \log\left(\frac{Q_t^i}{N_{\text{in}}}\right), \tag{4}$$

where X is neighborhood size, N_{in} is the number of intraCA cells, Q_t^i is the appearance frequency of binary triplet pattern i, and Q_t^i / N represents the probability of pattern i (note that i is a decimal representation of a bit pattern, e.g., "5" for "101"). After T_{in} steps, mean entropy $\overline{H_{\text{in}}}$ is calculated over another 100 time steps and used to determine the interaction radius R defined as:

$$R = \alpha\, \overline{H_{\text{in}}} = \text{int}(\alpha \langle H_{\text{in}}(t) \rangle), \tag{5}$$

where α is a scaling parameter and int is a round-down function. As mentioned, R determines the number of past transitions an ICA cell can look up to create a new rule at time $t+1$. Accordingly, two dynamics, rule-generating dynamics of ICA cells and intraCA dynamics, are coupled together for the evolution of ICA cells.

https://doi.org/10.25088/ComplexSystems.24.1.75

In this study, we fix the parameters as $N_{\text{in}} = 50$, $T_{\text{in}} = 200$, and $\alpha = 10$. The periodic boundary condition is adopted to calculate the time development of both ICA and intraCA cells. The spatiotemporal development of ICA is observed over 5000 steps.

3. Results

3.1 Emergence and Collapse of Complex and Periodic Patterns

In total, 20 runs were carried out with random initial conditions for both ICA cells and intraCA. In all 20 cases, the time development of ICA cells showed a spatiotemporal pattern similar to Figure 2(a). Roughly speaking, spatiotemporal patterns of ICA cells consist of periodic stripe regions and chaotic regions. The periodic stripe regions appear soon after starting from the random initial values. In Figure 2(a), chaotic regions are dominant and small periodic regions are found only in patches for the first 800 steps. However, a periodic region gradually extends, and chaotic regions were eventually wiped out at $t = 1000$. After this point, the whole system is in a globally stable phase where each cell remains in the same state for 120 steps. At $t = 1183$, however, a chaotic region reappears from one of the ICA cells and takes over the periodic regions. It eventually becomes predominant again from $t = 1400$. After $t = 1600$, the whole system repeats the tug-of-war between globally stable and globally chaotic phases. Both the duration of globally stable phases and the duration between two neighboring globally stable phases appeared to be random in all 20 cases.

The mechanism of the spatiotemporal pattern development can be explained as follows. As defined in equation (3), the principal dynamic of an ICA system is imitation of other cells. The appearance of the globally stable phase can be considered as a consequence of this dynamic. On the other hand, an ICA cell behaves randomly if it cannot find the same transition in neighboring cells within the interaction radius R. This dynamic accounts for the collapse of the globally stable phase at $t = 1183$. In the case of Figure 2(a), the collapse was triggered by the twenty-ninth imitating cellular automaton cell's state change from zero to one. In other words, the cell took the $101 \to 1$ transition at $t = 1182$, while $101 \to 0$ was adopted for a long period before that point. This is because the interaction radius R was zero, due to a small $\overline{H_{\text{in}}}$ value, and thus the cell filled a temporary rule table with all random bits. Accordingly, $101 \to 1$ is applied to compute the state at $t = 1183$, and this change propagates rightward due to the imitating behavior of ICA cells. Eventually it became a bundle of chaotic states and led to the collapse of the global stable phase.

https://doi.org/10.25088/ComplexSystems.24.1.75

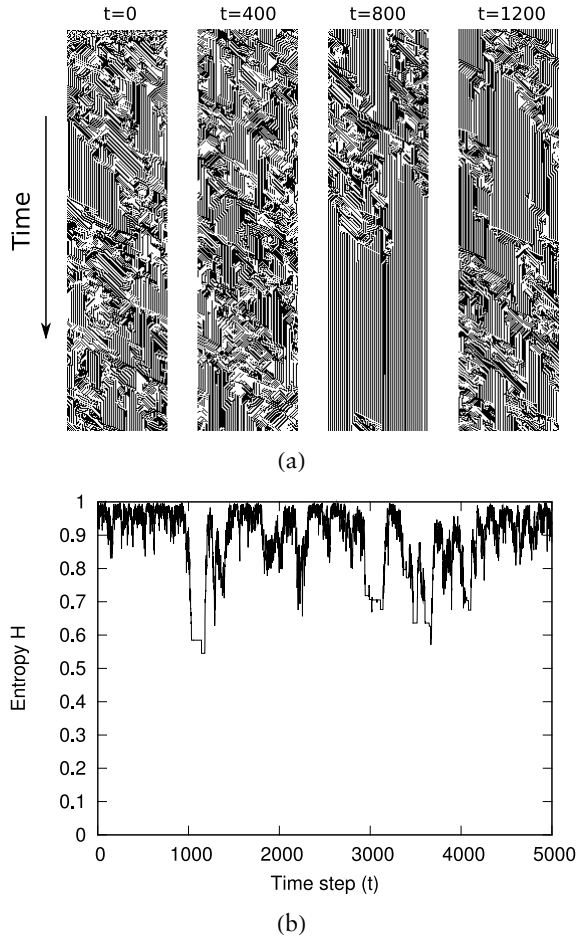

Figure 2. (a) A spatiotemporal pattern of ICA. The first 1600 time steps are shown. Black dots indicate the state is 1. A globally stable phase appears around $t = 1000$, followed by a sudden collapse at $t = 1200$. (b) The time course of the input entropy $H_{ex}(t)$ for (a). It fluctuates along with the time development and occasionally becomes constant when ICA are settled in a globally stable phase (e.g., at $t = 1000$ and 3000).

To quantify the development of the spatiotemporal pattern, input entropy $H_{ex}(t)$ for ICA cells is introduced. The definition of $H_{ex}(t)$ is the same as equation (4), but $H_{ex}(t)$ is calculated over a bit sequence of ICA cells at time t. This parameter works as an indicator of globally stable phases. If $H_{ex}(t)$ takes a constant value for a length of time, it means ICA are in a globally stable phase. As shown in Figure 3(b), ICA sporadically fall into a globally stable phase. Otherwise they os-

https://doi.org/10.25088/ComplexSystems.24.1.75

cillate at a higher range of $H_{ex}(t)$, which means ICA are dominated by chaotic phases.

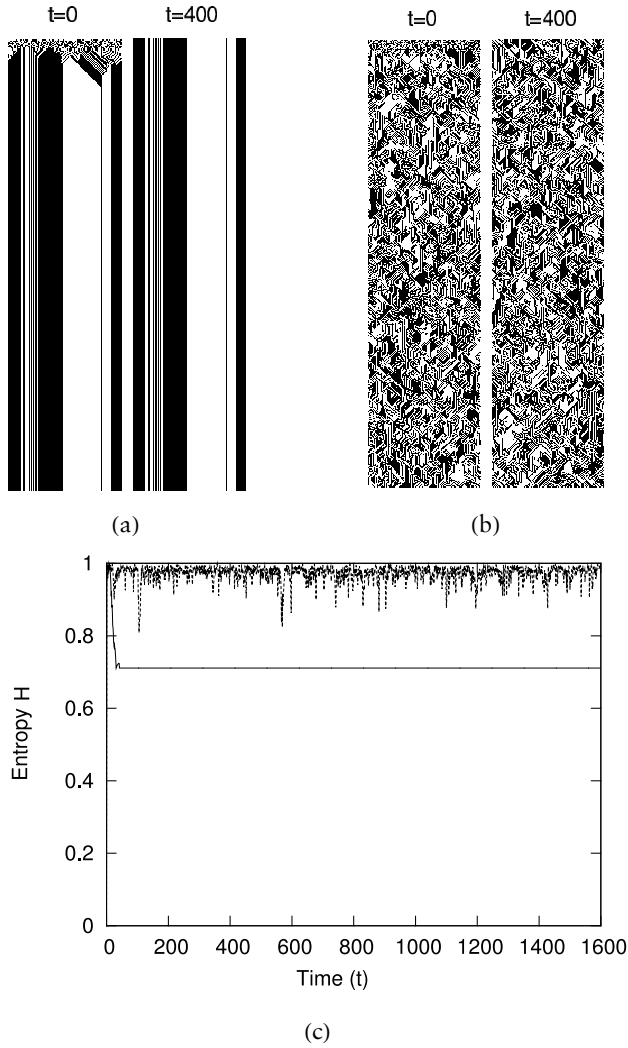

Figure 3. Spatiotemporal patterns of ICA in the case that the interaction radius R is (a) fixed or (b) randomly assigned. In all cases examined, the pattern ends up with a periodic pattern (when R is fixed) and a chaotic structureless pattern (when R is random). (c) The time course of the input entropy $H_{ex}(t)$ for (a) and (b). The fixed radius case (bold line) quickly settles down in a constant value, whereas the random case (dotted line) remains high throughout the entire period.

https://doi.org/10.25088/ComplexSystems.24.1.75

For comparison, two variants of ICA regarding interaction radius R are examined: R is either fixed or determined randomly. Note that the computation of intraCA is not required in these cases.

For the former case, R is fixed to a constant value ranging from 1 to 15 for all ICA cells throughout the whole time step. Twenty runs were carried out for each parameter value. In summary, observed spatiotemporal patterns were, in terms of Wolfram's classification of CA [8], mostly class 2 type (periodic pattern) and in rare cases, class 1 (all black or all white pattern) was observed. Once the system had fallen into either one of the two types, the pattern never changed afterward (Figure 3(a)). In the second case, when a random number from 1 to 15 was assigned for r of each ICA cell at every time step, there were no specific structures observed in all the cases (Figure 3(b)). Regarding the input entropy of these models, it settled down to a specific level after several hundreds of time steps in the first case and remained high throughout the time step in the second case (Figure 3(c)).

3.2 Emergence and Collapse of Clusters in Rule-Entropy Space

Figure 4(a–c) shows scatter plots of the input entropy $\overline{H_{\text{in}}}$ against the temporary rule number created by ICA cells at $t = 718$, 1118, and 1518. The data used for those plots is the same as Figure 2(a). Each circle in the plots corresponds to an ICA cell at a time step.

When the whole ICA system is in a chaotic phase, the distribution of ICA cells in the rule-entropy space appears to be random (Figure 4(a)). As the spatiotemporal pattern is organized into a globally stable phase, ICA cells form clusters in the rule-entropy space from $t = 1000$ (Figure 4(b)). Although the clusters are unstable and constantly fluctuating, ICA cells loosely keep the four clusters while they are in the globally stable phase. If the whole system falls out of the phase, the four clusters gradually collapse, and eventually ICA cells show random distribution again (Figure 4(c)).

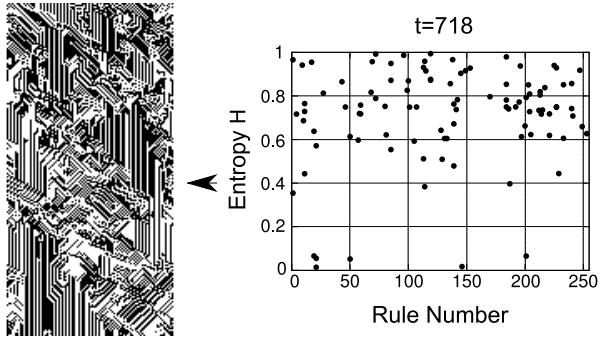

(a)

https://doi.org/10.25088/ComplexSystems.24.1.75

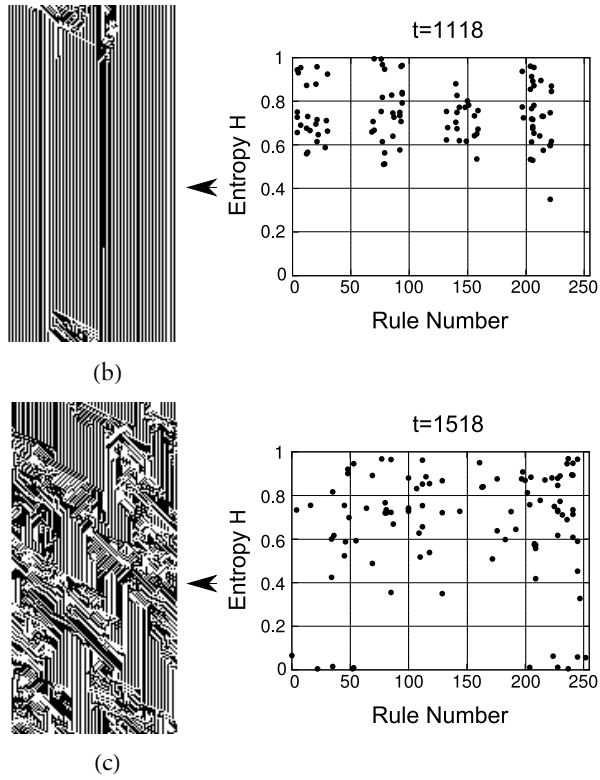

Figure 4. Emergence and collapse of clusters in rule-entropy space. (a)–(c) Plots of the mean input entropy $\overline{H_{\text{in}}}$ against rule numbers based on the data in Figure 2(a). Arrows by the spatiotemporal patterns on the left of the plots indicate the time step at which entropy values and rule numbers are sampled for the plots.

This result implies that ICA cells seem to develop some common element when they are in a globally stable phase, whereas temporary rules are created rather randomly during the chaotic phase. To further investigate this, we looked into components of the temporarily created rules, that is, transition patterns. A temporary rule, which is equivalent to a rule of ECA numbered from 0 to 255, has eight transition patterns from 000 to 111. These triplets are mapped onto either zero or one at the next time step. Considering that the main dynamic of the ICA system is to imitate transition patterns of other cells, information on transition patterns would work as another measure to investigate the underlying mechanism of ICA dynamics. In particular, we focused on how many cells have a specific transition from a triplet to one (e.g., 010 → 1) at each time step. Figure 5 shows time courses

https://doi.org/10.25088/ComplexSystems.24.1.75

of the number of cells that have the eight transition patterns. Each curve corresponds to a specific transition. Although it looks chaotic in the first half of the plot, transition patterns $010 \to 1$ and $101 \to 1$ show sharp increase and decrease, respectively, at $t = 1000$. The timing of this sharp change is exactly consistent with the appearance of the globally stable phase. As a result, almost all the ICA cells have $010 \to 1$ and $101 \to 0$ transitions during the stable phase. Having investigated all the 20 runs, we found that the dominance of $010 \to 1$ and the extinction of $101 \to 1$ were observed every time ICA fall into a globally stable phase. This fact accounts for two things about an ICA system: first, the stripe spatiotemporal pattern observed during a globally stable phase is created mainly by the two transitions, $010 \to 1$ and $101 \to 0$. An ICA cell using either transition remains itself in the same state. Thus, the combination of these two transitions … 01 010 101 … is the most stable solution for an ICA system. The longer the chain is, the more stable the pattern is. This explains why a globally stable phase mostly consists of the stripe bit pattern. Second, although there are four clusters observed in Figure 4(b), they are effectively one single cluster that consists of ICA cells that have both $010 \to 1$ and $101 \to 0$ transitions. As shown in Figure 5, transition patterns during a globally stable phase are mostly either $010 \to 1$ or $101 \to 0$. Accordingly, the only transitions an ICA cell can copy from other ICA cells are $010 \to 1$ and $101 \to 0$, and the other six transition patterns are filled with random bits. Because of the six transitions, the cluster virtually appears to be four in rule-entropy space.

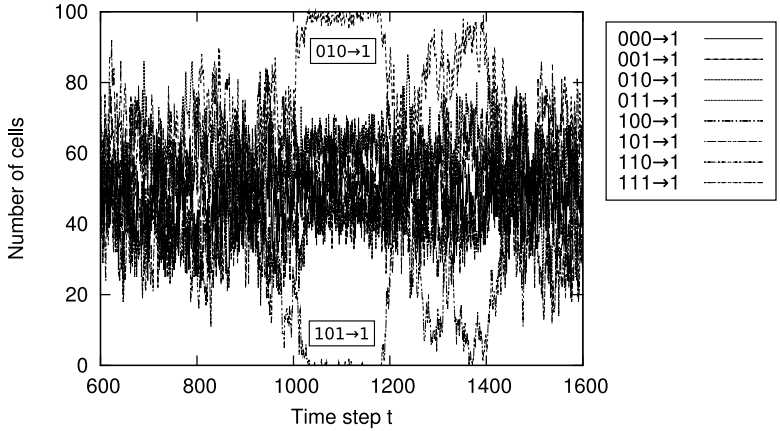

Figure 5. Time course of the number of cells that have a specific transition pattern in a temporary rule. All the ICA cells have $010 \to 1$ and $101 \to 0$ transitions, while ICA stay in a globally stable phase (from $t = 1000$ to 1200).

https://doi.org/10.25088/ComplexSystems.24.1.75

3.3 Effect of α on Global Spatiotemporal Patterns

The scaling parameter α in equation (5) determines the interaction radius R and thus can be considered as a crucial parameter for ICA dynamics. Spatiotemporal patterns of an ICA system are investigated when α is varied from 2 to 15. For each case, 10 runs were carried out. The mean and standard deviation (SD) of $H_{\mathrm{ex}}(t)$ are calculated to quantify the effect of α. Figure 6(a) and (b) show several patterns at different α and plots of the mean and SD against α, respectively.

The most remarkable thing regarding the effect of α is a phase transition between $\alpha = 6$ and 7. When $\alpha \leqq 6$, patterns looked chaotic, similarly to the case when R is determined randomly (Figure 3(b)). Globally stable phases did not appear at all. This can be confirmed from Figure 6(b), in which the mean remained high (due to chaotic patterns) and SD was low (no globally stable phases observed). In contrast, at $\alpha = 7$, periodic stable regions became dominant instead, and the area occupied with chaotic regions was rather small. Chaotic regions became more and more dominant as α increased. In fact, the mean entropy was increasing when $\alpha \geqq 7$ in Figure 6(b). In all cases above $\alpha \geqq 7$, observed patterns were basically similar to each other; that is, both periodic stable regions and chaotic regions were observed, and globally stable phases, which lasted over hundreds of time steps, appeared occasionally.

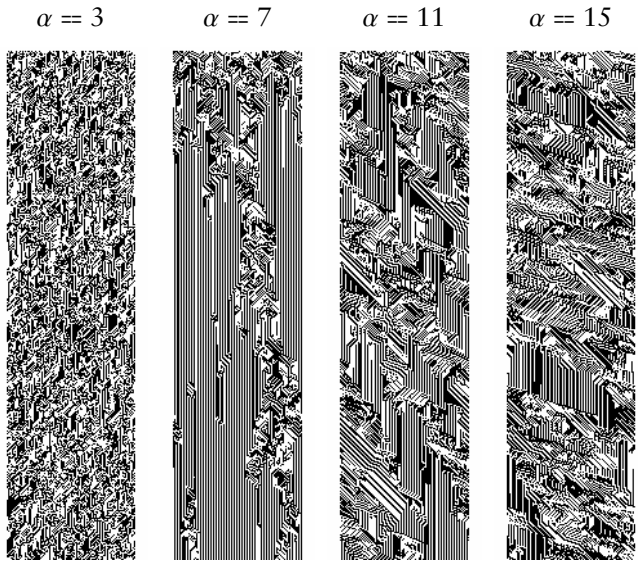

(a)

https://doi.org/10.25088/ComplexSystems.24.1.75

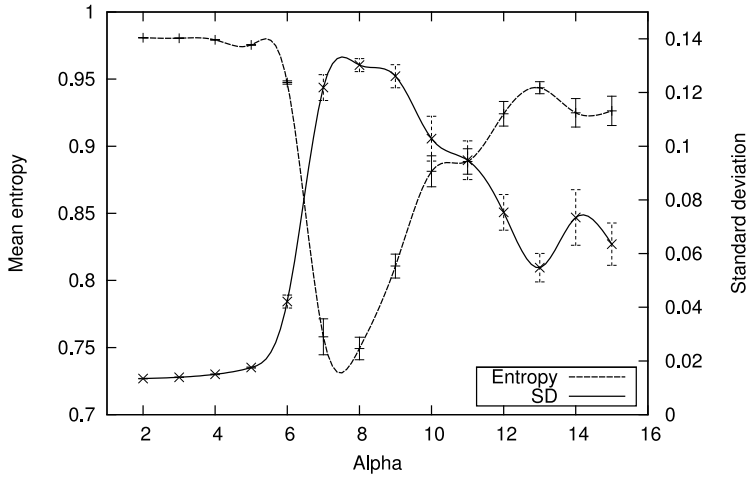

(b)

Figure 6. The effect of the interaction radius R on the spatiotemporal pattern. (a) Examples of the patterns at different R. The first 400 steps are shown. (b) A plot of the mean and standard deviation of input entropy $H_{\mathrm{ex}}(t)$ against the scaling parameter α.

3.4 Power Law in the Lifetime of Imitating Cellular Automata Cell

As mentioned in Section 3, ICA cells tend to remain in the same state once they are in a globally stable phase. Based on this fact, the length and frequency of duration that a cell remains in the same state (i.e., lifetime) were examined. Up to 10 000 steps of the spatiotemporal development data of ICA with $R = 10$ were used. The data from a variant of ICA where the interaction radius R is determined randomly (for short, random ICA) in Section 3.1 was analyzed for comparison. We did not distinguish the two states, 0 and 1, and focused simply on the duration of the same state.

A commonly used method to plot such data is to calculate a cumulative distribution function (CDF) that gives the probability of lifetime frequency greater than or equal to x, defined as [17]:

$$P(x) = \int_x^\infty p(x')\, dx', \tag{6}$$

where $p(x')$ is a probability of a lifetime length x'. Given that the original distribution follows a power law $p(x) = C\, x^{-\beta}$, it is known that the CDF of the distribution $P(x)$ also follows the power law with the exponent $\beta - 1$. The exponent of the original distribution can be calculated with the formula:

https://doi.org/10.25088/ComplexSystems.24.1.75

$$\beta = 1 + n \left[\sum_{i=1}^{n} \ln \frac{x_i}{x_{\min}} \right]^{-1}, \tag{7}$$

where n is the measured lifetime length and $x_{\min}$ is the minimum value of the lifetime. $x_{\min} = 1$ is used in this case. Figure 7 shows a log-log plot of the CDFs of normal ICA and ICA with random R against the frequency of lifetime x. Normal ICA follow a power-law distribution with the exponent 0.62 (thus $\beta = 1.62$), while random ICA do not. What makes the CDF of normal ICA different from that of random ICA are periodic stable periodic regions and global stable phases, which contribute to a longer lifetime. In fact, in length-frequency distribution plots (data not shown), the longest length of lifetime in random ICA was around 50 time steps, whereas that of ICA was around 5000 time steps, together with a long noisy tail in the end of the curve.

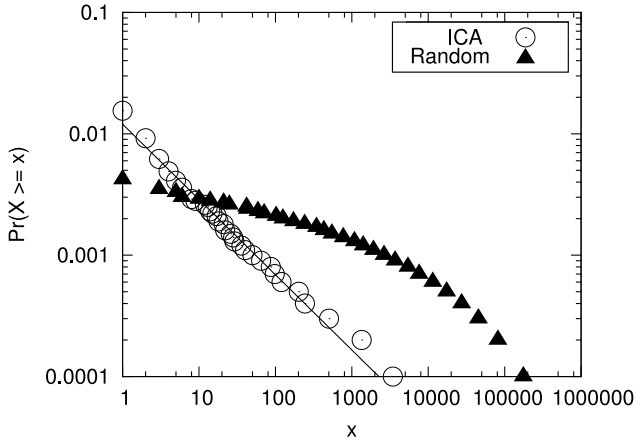

Figure 7. A log-log plot of the cumulative distribution function of ICA cell lifetime. Normal ICA follow a power law with the exponent $\beta = 1.62$.

4. Discussion and Conclusion

We presented a model of mutually imitating agents based on cellular automata (CA), called imitating cellular automata (ICA). Despite the simple design, the spatiotemporal pattern of ICA showed complex class 3-like behavior mixed with chaotic and periodic stable patterns. It has been observed that globally stable phases, in which each ICA cell keeps the same state, occasionally emerge and eventually collapse after a certain period of time. It was found that such complex pat-

https://doi.org/10.25088/ComplexSystems.24.1.75

terns were due to the coupling of the imitating (rule-generating) dynamics and the intra-agent dynamics. In fact, when the intra-agent dynamics were absent, the patterns were totally periodic or complex. In other words, the intra-agent dynamics coordinate the complexity level of a system at a moderate level. Without those dynamics, a system will fall into stable states or utter chaos. As a result of the coordination, the ICA dynamics exhibit the power-law relationship in the lifetime of cell states.

Numerous complex system models have been proposed to answer how a system can maintain the complexity of the system at an appropriate level, the so-called "edge of chaos" state [18]. Some models adopt two coupled dynamics to achieve complex emergent systems. A classical example of such a model is Turing's chemical morphogenesis [19], and a more recent example is self-organized criticality (SOC) models, first proposed by Bak [20]. It should be mentioned that the critical difference between ICA dynamics and the preceding models is the interdependency of the employed dynamics. In previously proposed models, two dynamics employed to model a system are independently defined. For example, in the forest fire model by Drossel and Schwabl [21], two dynamics, the tree growth probability p and the lightning probability f, are defined independently and fixed throughout the computation. On the other hand, in the ICA model, the imitating dynamics determine the "shape" of the intra-agent dynamics, that is, a rule used for the dynamics, and an outcome of the intra-agent dynamics crucially affects the formation of the imitating dynamics. In some cases it drastically changes the direction of future development of ICA system, as illustrated by the collapse of a global stable phase. In other words, two dynamics employed for ICA are built up from the interactions to another dynamic as well as with other ICA cells on an ad hoc basis. As a result, a system with such coupled dynamics does not end up in utter chaos, but in reality the interrelated dynamics allow the system to take a wide range of states and also allow globally stable phases to emerge.

In addition to the interrelated dynamics, it should be pointed out that random bit fillings also undertake an important role for the emergence of complex spatiotemporal patterns. If an ICA cell has blanks in a temporary rule table, the cell fills them with random bits. When ICA are dominated by chaotic regions, an ICA cell can copy various kinds of transition patterns from the neighborhood cells, and only a few blanks in a temporary rule are filled with random bits. In this case, the dynamic that determines the next state of the ICA cell is mostly governed by the imitating behavior, and the effect of randomly determined rules is rather suppressed. When periodic stable regions are dominant, on the other hand, observed transition patterns are

https://doi.org/10.25088/ComplexSystems.24.1.75

mostly either $010 \to 1$ or $101 \to 0$, and the other six transition patterns are filled with random bits, which increases the chance that chaotic regions become larger. In some rare cases, this gives a low $\overline{H_{\text{in}}}$ value and it leads the system to escape out of a globally stable phase, as we showed in Section 3. Thus, being intermediated by the intra-agent dynamics, blanks in a temporary rule table work as a "buffer" for the whole ICA system to avoid being trapped in extreme cases, equilibrium, or chaotic states. In fact, complex patterns were not observed at all when blanks were filled in a deterministic way (e.g., all the blanks were filled with zero; data not shown).

Although the model presented in this paper is quite simple, it displayed complex patterns robustly when $R \geqq 7$. The combination of the imitating behavior, the random behavior, and the intra-agent dynamics provided flexibility to the whole dynamics. Arguably, the robustness to the parameter change is one of the consequences of the combination, which enabled the system to self-organize the complex patterns. We just examined the simplest case. If the parameter space becomes larger, for example if ICA cells can take more than two states, ICA would show more complex and interesting spatiotemporal patterns. We also speculate that the basic design of the ICA system, inspired from a fundamental behavior of living systems, would turn out to be useful to construct a model of natural "lifelike" phenomena, such as animal population dynamics and stock market dynamics.

Acknowledgments

The author wishes to thank Yukio-Pegio Gunji and Stefan Artmann for their critical comments and thank the Lord Kelvin Adam Smith Research Fellowship for financial support.

References

[1] T. R. Zentall, "Imitation: Definitions, Evidence, and Mechanisms," *Animal Cognition*, **9**(4), 2006 pp. 335–353. doi:10.1007/s10071-006-0039-2.

[2] G. Rizzolatti and L. Craighero, "The Mirror-Neuron System," *Annual Review of Neuroscience*, **27**, 2004 pp. 169–192.

[3] O. Tchernichovski and F. Nottebohm, "Social Inhibition of Song Imitation among Sibling Male Zebra Finches," *Proceedings of the National Academy of Sciences of the United States of America*, **95**(15), 1998 pp. 8951–8956.

https://doi.org/10.25088/ComplexSystems.24.1.75

[4] G. Gergely, H. Bekkering, and I. Király, "Developmental Psychology: Rational Imitation in Preverbal Infants," *Nature*, **415**(755), 2002 p. 755. doi:10.1038/415755a.

[5] J. Suzuki and K. Kaneko, "Imitation Games," *Physica D: Nonlinear Phenomena*, **75**(1–3), 1994 pp. 328–342. doi:10.1016/0167-2789(94)90291-7.

[6] Y.-M. Wei, S.-J. Ying, Y. Fan, and B.-H. Wang, "The Cellular Automaton Model of Investment Behavior in the Stock Market," *Physica A: Statistical Mechanics and Its Applications*, **325**(3–4), 2003 pp. 507–516. doi:10.1016/S0378-4371(03)00144-4.

[7] G. Qiu, D. Kandhai, and P. M. A. Sloot, "Understanding the Complex Dynamics of Stock Markets through Cellular Automata," *Physical Review E*, **75**, 2007 p. 046116. doi:10.1103/PhysRevE.75.046116.

[8] S. Wolfram, *A New Kind of Science*, Champaign, IL: Wolfram Media, Inc., 2002.

[9] O. Mazonka, "Bit Copying: The Ultimate Computational Simplicity," *Complex Systems*, **19**(3), 2013 pp. 263–285. http://www.complex-systems.com/pdf/19-3-5.pdf.

[10] A. Adamatzky and A. Wuensche, "On Creativity and Elementary Cellular Automata," *Complex Systems*, **22**(4), 2013 pp. 361–375. http://www.complex-systems.com/pdf/22-4-2.pdf.

[11] J. P. Crutchfield and J. E. Hanson, "Turbulent Pattern Bases for Cellular Automata," *Physica D: Nonlinear Phenomena*, **69**(3–4), 1993 pp. 279–301. doi:10.1016/0167-2789(93)90092-F.

[12] L. B. Kier, P. G. Seybold, and C.-K. Cheng, *Modeling Chemical Systems Using Cellular Automata*, Dordrecht: Springer, 2005.

[13] G. B. Ermentrout and L. Edelstein-Keshet, "Cellular Automata Approaches to Biological Modeling," *Journal of Theoretical Biology*, **160**(1), 1993 pp. 97–133. doi:10.1006/jtbi.1993.1007.

[14] A. Smirnoff, S. J. Paradis, and R. Boivin, "Generalizing Surficial Geological Maps for Scale Change: ArcGIS Tools vs. Cellular Automata Model," *Computers & Geosciences*, **34**(11), 2008 pp. 1550–1568. doi:10.1016/j.cageo.2007.10.013.

[15] H. Nakanishi, "Cellular Automaton Model of Earthquakes with Deterministic Dynamics," *Physical Review A*, **41**(12), 1990 pp. 7086–7089. doi:10.1103/PhysRevA.41.7086.

[16] A. Wuensche, "Classifying Cellular Automata Automatically: Finding Gliders, Filtering, and Relating Space-Time Patterns, Attractor Basins, and the Z Parameter," *Complexity* **4**(3), 1999 pp. 47–66. doi:10.1002/(SICI)1099-0526(199901/02)4:3<47::AID-CPLX9>3.0.CO;2-V.

[17] M. E. J. Newman, "Power Laws, Pareto Distributions and Zipf's Law," *Contemporary Physics*, **46**(5), 2005 pp. 323–351. doi:10.1080/00107510500052444.

https://doi.org/10.25088/ComplexSystems.24.1.75

[18] C. G. Langton, "Computation at the Edge of Chaos: Phase Transitions and Emergent Computation," *Physica D: Nonlinear Phenomena*, 42(1–3), 1990 pp. 12–37. doi:10.1016/0167-2789(90)90064-V.

[19] A. M. Turing, "The Chemical Basis of Morphogenesis," *Philosophical Transactions of the Royal Society B: Biological Sciences*, **237**, 1952 pp. 37–72. doi:10.1098/rstb.1952.0012.

[20] P. Bak, *How Nature Works: The Science of Self-Organized Criticality*, New York: Copernicus, 1996.

[21] B. Drossel and F. Schwabl, "Self-Organized Critical Forest-Fire Model," *Physical Review Letters*, **69**(11), 1992 pp. 1629–1632. doi:10.1103/PhysRevLett.69.1629.

https://doi.org/10.25088/ComplexSystems.24.1.75